



Metal Oxides Based Hydrogen Sensor Works at Room Temperature

Salim F. Bamsaoud^{1,2,3*}, R. C. Aiyer¹ and S. W. Gosavi¹

¹*Microwave and Thin Film Lab, Department of Physics, University of Pune, India.*

²*Department of Physics, Faculty of Science, Hadhramout University, Mukalla, Yemen.*

³*Department of Architecture and Environmental Engineering, Faculty of Engineering, University of Science and Technology, Hadhramout, Yemen.*

Authors' contributions

This work was carried out in collaboration among all authors. Author SFB performed the experimental studies and wrote the first draft of the manuscript. Author RCA wrote the protocol and managed the analyses of the study. Author SWG performed the characterization experiments of materials and managed the literature searches. All authors read and approved the final manuscript.

Article Information

DOI: 10.9734/JENRR/2020/v5i430156

Editor(s):

(1) Dr. Huan-Liang Tsai, Da-Yeh University, Taiwan.

Reviewers:

(1) Seyed Amirabbas Zakaria, Chemistry and Chemical Engineering Research Center of Iran, Iran.

(2) Jamal M. Rzaij, University of Anbar, Iraq.

Complete Peer review History: <http://www.sdiarticle4.com/review-history/58663>

Original Research Article

Received 15 June 2020
Accepted 22 August 2020
Published 02 September 2020

ABSTRACT

Tin chloride and Palladium chloride were used to fabricate H₂ sensor based on PdO, SnO₂ and PdO_x functionalized SnO₂ nanoparticles. These sensors were fabricated by spin coating technique using single step thermal decomposition method (SSTD) with annealing temperature of 550°C. The chemical composition and microstructure of the obtained samples were characterized by using X-ray diffraction, UV-VIS spectra, transmission electron microscopy and energy-dispersive X-ray spectroscopy. The sensing characteristic of sensors was investigated at different operation temperatures 25, 50 and 80°C. Results showed that PdO_x-SnO₂ sensor exhibited excellent sensing performance to H₂ at room temperature (RT). When the operating temperature was 50°C, the detection limit towards H₂ was 0.5 ppm with ultrafast response and recovery time. In addition, the sensor exhibited excellent stability and repeatability at different relative humidity with a high selectivity to H₂ detection against CO, CO₂, LPG, acetone, methanol and ethanol vapor.

*Corresponding author: E-mail: saalem88@yahoo.com;

Keywords: Tin oxide; palladium; sensor; hydrogen; room temperature.

1. INTRODUCTION

The advent of hydrogen age has been growing since hydrogen emerged as a new source of green energy. Currently, the great interest in developing hydrogen sensors has come due to the involvement of hydrogen in many applications such as semiconductor processing (microelectronics, chemical and petroleum refining), fuel cells, rocket fuels for spacecraft, neon and xenon production, biomedical applications, and other industrial applications [1]. Hydrogen is highly explosive in air when the concentrations exceeds 4%; therefore, sensor having particular specifications such as high sensitivity, detection of lower concentration, fast response and recovery time could overcome the technical challenges like hydrogen storage and safety [2]. Thus, the utilization of H₂ sensors to notify the leaks and to monitor the gas during manufacturing is of great importance.

Tin oxide compared to other metal oxides based hydrogen sensor was widely used due to their promising results in gas sensor application [3,4]. One of the main challenges in fabricating room temperature gas sensors based metal oxide is the selection of the used functional materials with proper control of all the factors that have explicit effect in sensing mechanism.

Hydrogen sensors works at room temperature were reported by many researchers [4–16]. They have done an excellent work to fabricate hydrogen sensor using highly cost with comparably lengthy fabrication methods. However, a preparation method with a low cost, uncomplicated preparation steps and no lithograph, are always recommended at manufacturing point of view. The highest reproducibility of sensor could be achieved by choosing proper preparation method with simple and fewer stages in finalizing the sensor.

In this study, we report one-step with vacuum-less synthesis method to fabricate nanostructured SnO₂, PdO and PdO_x-SnO₂ hydrogen sensor. Comprising study in sensing performance at lower operating temperature, including the effect of humidity in sensor response and selectivity to hydrogen against different gases, were studied.

2. EXPERIMENTAL TECHNIQUES

Tin oxide, palladium oxide and palladium oxide-tin oxide films were prepared by the single step

thermal decomposition method (SSTD) using metal chlorides [3]. The three different chloride solutions (PdCl₂, SnCl₂, and SnCl₂+PdCl₂) were prepared using acetic acid as a solvent. For SnO₂ (or PdO), the solution was prepared by adding 2 g (metal chloride) to 8 ml of distilled water and stirred for half an hour. Then 4 ml of glacial acetic acid was added into chloride solution and stirred again for 1 h at 90°C to obtain a transparent solution. The films were obtained by spin coating 0.5 ml of the above prepared solution on soda lime glass. The dried films were then annealed in the furnace at 550°C for 40 min with a heating rate of 5°C/min [13], to get an adherent film. For PdO_x-SnO₂ films, PdCl₂ (3% wt) was mixed with SnCl₂ (97%) powder. 2 g of the mixed powder was added to 8 ml and followed by the same preparation method of SnO₂ and PdO films. Film thickness measurements were taken using profilometry (P-16 + TM, KLA-Tencor, USA). The error on these measurements is estimated to be ±30 Å.

The fabrication of sensors can be briefly described as follow: Silver was printed on a 1.5×0.5 cm² of the annealed film using screen printing technique (as a part of simplicity in sensor fabricating). The printed electrodes were allowed to dry for 1 hour under an infrared lamp (IR) and copper wires were soldered easily. The sensors were subjected to no further treatments and they are ready to use. Fig. 1 shows photograph of the fabricated metal oxide sensor. For sensor circuit, the prepared film connected in series with a 8 × 10³Ω reference resistor and 1.5 V cell, was built in an electronic printed circuit board of dimension (6 × 1 cm²). The integrated circuit was arranged to be attached to a multimeter for measuring the voltage drop across the reference resistance.

The small angle X-ray diffraction (XRD) of the annealed films was carried out using X-ray diffractometer (Bruker AXS D8 Advance model) using Cu K_α radiation (λ = 1.5418Å) at angle of 1°. UV-VIS spectra of films deposited on glass substrate were recorded on spectrophotometer (Jasco V-670) and the microstructure analysis was carried out using transmittance electron microscope (JEOL, Model JSM -6360A). For transmission electron microscopy (TEM), the collected powder was scraped from samples (films) and dispersed in acetone. The elemental analyses were examined using energy-dispersive X-ray spectroscopy (EDS) with an X-ray analyzer integrated with a TEM instrument.

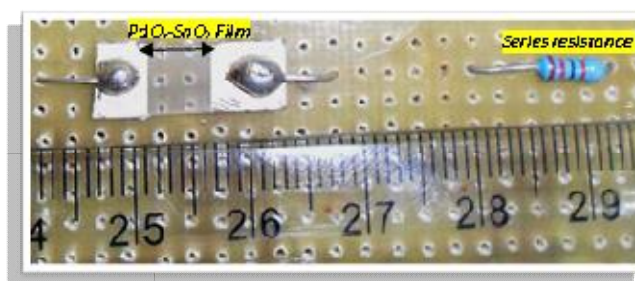


Fig. 1. Photograph of nanostructured PdO_x-SnO₂ room temperature hydrogen sensor

The sensing characterization was carried out using a static system [3,13]. The sample was placed in a stainless steel base plate with several electrical feed-troughs and gas inlet. A 26 liter glass dome was placed on the base plate to form air tight chamber. For response measurements, a dc power supply of 1.5 V was applied between our sensor and the $8 \times 10^3 \Omega$ resistance (reference resistance). Voltage drop on the reference resistance was measured. For variation of sample temperature, a heater located separately on the back of the substrate. Sensor response magnitude was defined as ($R_s = R_{air}/R_{gas}$), R_{air} and R_{gas} are sensor resistance in the presence and absence of hydrogen respectively. The resistance of sensor was determining using half bridge method by measuring the voltage drops across the reference resistance. We define the response time as the time taken for the sensor resistance to undergo a 90% variation with respect to its equilibrium value and recovery time as the time taken to achieve 10% variation to reach its initial value in air after the removal of H₂. Relative humidity (RH %) inside the test chamber was controlled by passing humid or dry air in the test chamber. The change in RH% was directly measured using a calibrated hygrometer (DIEHLThermotord Hgro).

3. RESULTS AND DISCUSSION

3.1 Material Characterizations

The deposited films, after subjected to thermal process, were homogeneous, uniform and showed an excellent adhesion to soda-lime glass substrate. Thickness of the films was found to be 250-300 nm.

Fig. 2a illustrated the XRD pattern of the oxides deposited on soda-lime glass substrate. From the recorded XRD data (Fig. 2a), it can be seen

that all the diffraction peaks of films prepared from SnCl₂ solutions were well indexed to the tetragonal SnO₂ structure (JCPDS card, No.42-1147). The X-Ray analysis, for film deposited using PdCl₂ solution, indicated that film is polycrystalline and the diffraction peak were indexed to the (111) reflection of a tetragonal structure of PdO (JCPDS card No. 72-1147). The recorded diffraction peak for PdO was located at $2\theta = 33.9$.

UV-VIS spectra (Fig. 2b) of all films (SnO₂, PdO and PdO_x-SnO₂), showed a single narrow optical absorption "peak". The absorption peak was found to be located between 278-295 nm. The UV-Vis absorption peak of SnO₂ located at 295 nm (the calculated optical energy band gap is 4.2 eV). For PdO sample, the UV-Vis absorption peak was found to be at 278 nm. With around 3% of Pd that PdO_x-SnO₂ film contained, the absorption spectra of this film showed a blue shift and the peak was found to be at 280 nm with calculated optical band gap of ~ 4.48 eV.

Fig. 3(a), (b) and (c) shows the TEM images of pristine SnO₂, PdO and PdO_x-SnO₂ sample. The SAED patterns (inset Fig. 3) of SnO₂, PdO and PdO_x-SnO₂ revealed that the materials were found to be of poly-crystalline structures. The TEM of pristine SnO₂ (Fig. 3a) shows nearly spherical particles of 5 nm and some particles with bigger size of 10-15 nm. This TEM results of powder obtained from SnO₂ film confirmed the bimodal distribution that was seen by atomic force microscopy (AFM) for SnO₂ films prepared by the SSTD method [13]. This distribution (5 nm particles distributed on the surface of nanoparticles having bigger size of 10-15 nm) could not be clearly seen by TEM due to, probably, the disturbance of film morphology when scraping process took place to obtain sample. Fig. 3b shows that the particle size of PdO is around 2-3 nm. Also, the TEM image of PdO_x-SnO₂ reveals that the particle size is 2-5

nm. Moreover, the particles shape is identical which could be because of palladium that had an influence on particle size of SnO₂ by keeping the particles identical. Such results, (influencing in SnO₂ particle size with palladium) were noted by Tan et al. [17]. They reported that the results could be due to the presence of Pd additive that modify the growth kinetic of SnO₂ nanoparticles. Similarly, Luo et al. [18] and Fardindoost et al. [7] observed an influence in particle size of tungsten (W) when Cerium (Ce) and Palladium (Pd) added to tungsten. They

suggested that due to the lower ionic radius of W+6 (56 pm) comparing to the ionic radii of the additive (Ce and Pd) the catalyst particles may get accumulated in the grain boundaries of tungsten. Because of the accumulation, the grain growth during heat treatment was prevented. In our case, the ionic radius of Sn⁴⁺ is somehow smaller (71 pm) than Pd ion (78 pm) and it is probably happening that Pd is accumulated in the grain boundaries of tin preventing the grain growth during thermal treatment.

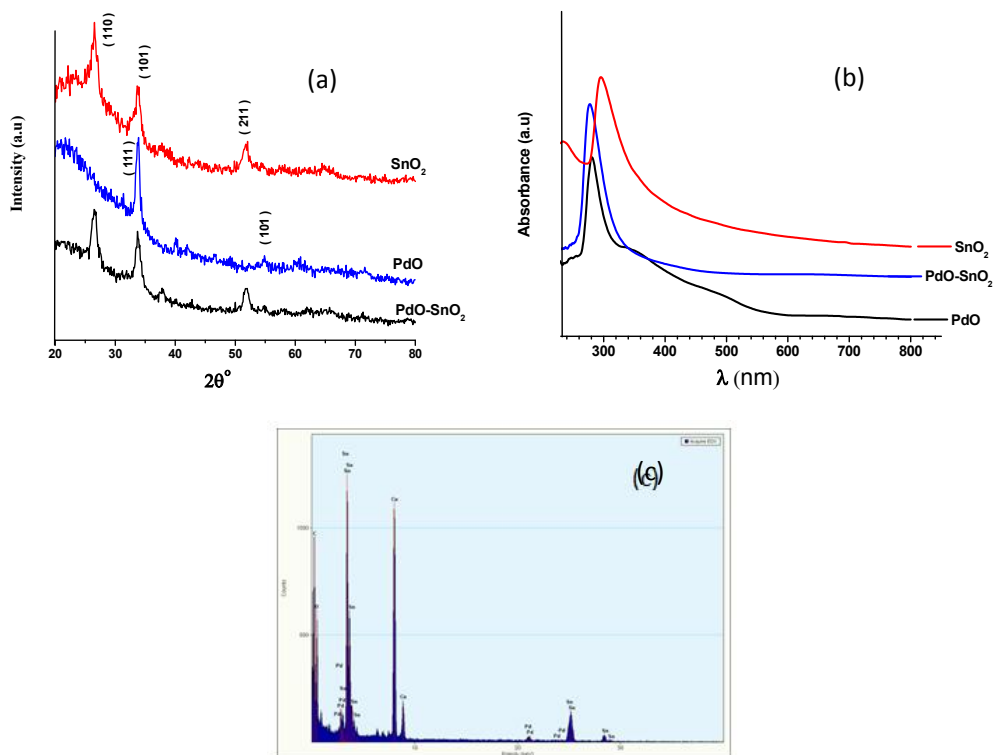


Fig. 2. (a) X-ray diffractogram, (b) UV-Vis of SnO₂, PdO and PdO_x-SnO₂ film deposited on soda-lime glass substrate and (c) EDS data of PdO_x-SnO₂

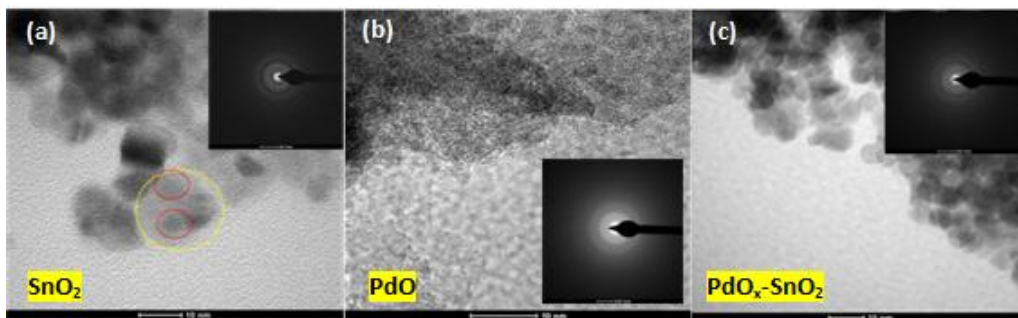


Fig. 3. TEM images of (a) SnO₂,(b) PdO and (c) PdO_x-SnO₂ samples

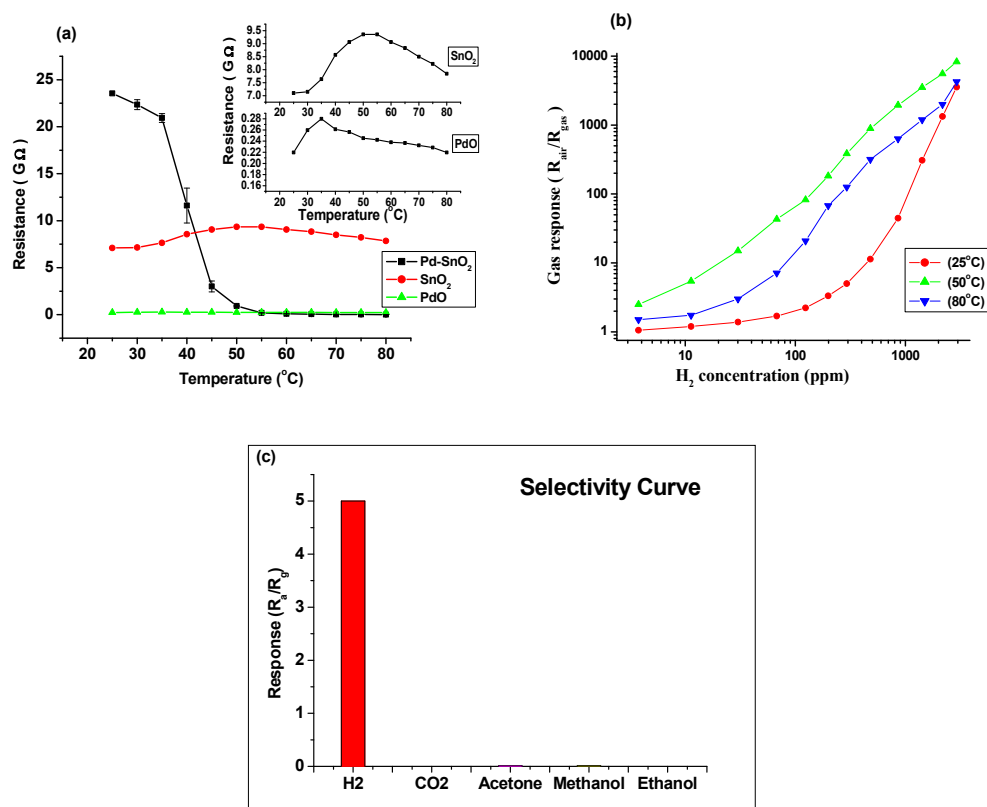


Fig. 4. (a) Variation of sensor resistance with temperature for SnO₂, PdO and PdO_x-SnO₂, (b) Response variation of H₂ concentration (4-3000 ppm) for PdO_x-SnO₂ sensor at operating temperatures of RT, 50 and 80°C, (c) Selectivity curve at 50°C for 3000 ppm of gas/vapor

3.2 Variation of Sensor Resistance with Respect to Temperature

Fig. 4 shows a typical variation in sensors resistance of SnO₂, PdO and PdO_x-SnO₂ with temperature. The resistance of sensor was recorded at temperature range starts from 25°C to 80°C. The resistance value of pristine SnO₂ film increased from 7×10^9 Ohms at 25°C to reach maximum value of 8.6×10^9 ohms at 50°C and it reduced with further increasing in temperature to reach 4×10^9 ohms at 80°C. Similarly, the resistance of pristine PdO film was recorded to increase for 0.22×10^9 ohms at 25°C to reach its maximum value of 0.28×10^9 ohms at 35°C. And with further increasing in sensor temperature the resistance decreased to reach the value of 0.21×10^9 ohms at 80°C. The temperature at which the sample changes its behavior from positive temperature coefficient (PTC) to negative temperature coefficient (NTC) was 50°C and 35°C for pristine samples of SnO₂ and PdO respectively. The noted change, PTC to

NTC, in sample resistance was observed by Ansari et al. [19]. This observed peak value (inset Fig. 4), at which highest resistance of SnO₂ film was recorded, noted to be reduced and shifted with Relative Humidity (RH %) [13]. Unlikely, PdO_x-SnO₂ film have no initial PTC behavior with temperature. The sample showed continuous reduction in resistance values with increasing in sensor temperature. The resistance value of PdO_x-SnO₂ film noted to be higher than that of pristine sample. It reached value of $\sim 23 \times 10^9$ ohms at temperature of 25°C. When sample reaches 35°C a sudden sharp decreasing in sensor resistance (decreases by 96% of maximum value) was observed. Also, no remarkable decreasing in sensor resistance above 55°C was recorded. It can be noted that the higher resistance of PdO_x-SnO₂ film may be due to some interface barriers created unknowingly in PdO_x doped SnO₂ sensor. The PTC behavior that observed for SnO₂ and PdO was due to desorption of water [19]. This fact revealed that, PdO_x dopant is responsible for the

continues reduction in $\text{PdO}_x\text{-SnO}_2$ sample resistance and it probably prevented water molecules to get adsorbed at the surface of SnO_2 film at lower temperature (25-50°C). The sudden relatively increasing of charge carrier in $\text{PdO}_x\text{-SnO}_2$ film indicates that an energy of KT ($T=50^\circ\text{C}$) is relatively enough to activate electrons at some certain energy level in the band gap to participate in electrical conductivity of $\text{PdO}_x\text{-SnO}_2$. It can be noted that $\text{PdO}_x\text{-SnO}_2$ film showed a significant increase in conductivity by 96% at (35-50°C) while conductivity of pristine SnO_2 and PdO films increased by only 12% and 20% respectively at 80°C.

3.3 Hydrogen Sensing Measurements

The sensors response was tested towards hydrogen concentration (3-3000 ppm). For SnO_2 as well as PdO sensors at operating temperatures (25, 50 and 80°C), showed no gas response towards H_2 . The sensors response noted when sensor temperature approach 100°C and the highest response of SnO_2 and PdO sensors towards 300 ppm of hydrogen was noted to be 24 and 11 at temperature of 260°C [3] and 200°C, respectively. It could be useful to mention that SnO_2 and PdO sensors, when tested individually for hydrogen at operating temperature above 100°C, showed an n type behavior i.e. the resistance decreases when hydrogen is exposed to sensor surface.

Fig. 4b depicts sensor performers of $\text{PdO}_x\text{-SnO}_2$ films at different operating temperatures (25, 50 and 80°C). The vertical axis presented the

calculated response ($R_{\text{air}}/R_{\text{H}_2}$) of the sensor. At room temperature the response of sensor increased slowly towards hydrogen concentration for the concentration range of > 3 to 100 ppm. The sensor showed more or less a linear response when tested for higher than 100 ppm concentration. Additionally, the convex behavior of sensor response indicated the ability of sensor to work for higher concentration more than 3000 ppm. At sensor working temperature of 50°C, a remarkable increasing in response was observed with best linearity in sensor response curve. When the operating temperature of sensor increased to 80°C, a reduction of around 40% in sensor response was noted comparing to the response of sensor at 50°C. The temperature (50°C), at which the sensor showed the highest response, was considered to be the optimal operating temperature of the sensor.

$\text{PdO}_x\text{-SnO}_2$ sensor, when was tested individually for 3000 ppm of different gases viz. LPG, CO_2 , acetone, ethanol and methanol vapors (Fig. 4c), showed practically no response towards these gases at the studied operating temperatures (25-80°C). However, the sensor showed unexpected behavior to carbon monoxide (CO) at 25°C. An increase in sensor resistance was observed when CO was exposed which is exactly opposite to what sensor showed when hydrogen is exposed at same sensor temperature. The reaction of CO with our sensor ($\text{PdO}_x\text{-SnO}_2$) revealed that there is somewhat an oxidization process-like was taking place at the surface. The sensing properties of this sensor against CO, and the reason behind the expected reaction that increases the sensor resistance, are under study.

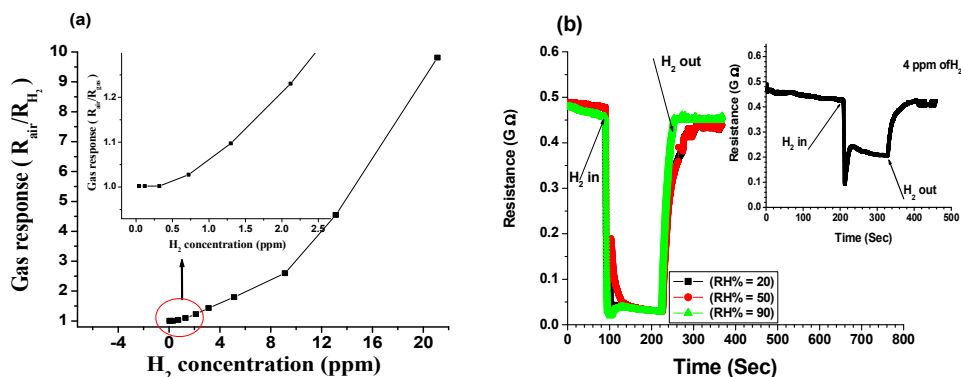


Fig. 5. (a) Response variation with H_2 concentration (0.03-20 ppm) and (b) response of 100 ppm H_2 at 50°C with different RH% for Pd doped SnO_2 sensor

Fig. 5a depicted the variation of sensor response of PdO_x-SnO₂ towards lower hydrogen concentration (0.04 to 0.3 ppm). Starting with the smallest concentration (0.04 ppm) the sensor showed no change in sensor resistance before and after hydrogen injected. The change in the resistance of sensor was clearly occurred when the concentration of hydrogen reached 0.5 ppm. Therefore, 0.5 ppm of hydrogen concentration (see inset of Fig. 5), considered as the detection limit of PdO_x-SnO₂ sensor. The sensor response of detection limit of hydrogen gas was found to be ($R_{air}/R_{gas} = 1.03$).

The response and recovery times of PdO_x-SnO₂ films at the optimal operating temperature (50°C) in presence of different RH% (20-90%), are presented in Fig. 5b. The study was done for 100 ppm of hydrogen. The inset presented response and recovery time of the sensor for 4 ppm. The PdO_x-SnO₂ sensor showed no remarkable effect on the response of 100 ppm of hydrogen in presence of different relative humidity. This effect of humidity on sensor response was studied at tested temperatures (25-80°C) and there was no effect observed on sensor response. At RT the sensor shows slight increasing in resistance value of about 3% for RH=90%. This increase in resistance might be due to some SnO₂ surface available with no Pd catalyst exist on PdO_x-SnO₂ film. The response and recovery time, of the sensor measured for 100 ppm at room temperature were found to be 50 and 120 sec respectively. And at the optimal operating temperature of the sensor (50°C), the response and recovery time were 4 and 9 sec respectively. While at 80°C the response and recovery time were found to be 3 and 6 sec.

3.4 Discussion

The XRD data for films prepared from PdCl₂-SnCl₂ solution revealed that all the peaks are related to the tetragonal structure of SnO₂ with no shift in peaks position. The peak corresponding to (111) is having the highest intensity and located at $2\theta = 33.6^\circ$. Moreover, no impurity phases correlated with Pd, PdO or PdO₂ in the X-ray patterns of the PdO_x-SnO₂ samples. The additive Pd was detected by EDS (Fig. 2c) and it was probably small enough to be detected by XRD.

The observed blue shift in the optical band gap energy (UV-Vis) of PdO_x-SnO₂, with respect to that of bulk SnO₂, might be due to smaller-sized particles and/or morphology. The single narrow

absorption peaks that UV-Vis revealed, can be explained by what Dharmadhikari et al reported [20]. They reported that nanoclusters having sizes comparable to that of the bulk Bohr exciton radius (a_B), exhibit discrete electron energy levels with high oscillator strength. The effect of quantum confinement for semiconductor is expected as indicated by the shift of absorption edge/peak to higher energy when the particle size decreases [20,21].

When Tan et al. [17] investigate their PdO_x-SnO₂ system (2.5% of Pd doped SnO₂ fired at 400°C) using X-ray photoelectron spectroscopy (XPS), two chemical states Pd²⁺ and Pd⁴⁺ which are related to PdO and PdO₂, were confirmed. They reported that XRD data of their PdO_x-SnO₂ film showed no impurities phases correlated with Pd. Similarly, when Zhang et al. [22] used stannous chloride and palladium chloride to deposit PdO_x-SnO₂ film, they confirmed the existence of PdO in their films by XPS. The XRD data of their film showed no peaks related to Pd in nanofibers PdO_x-SnO₂ film annealed at 450°C. In the present study, although XRD data for PdO_x-SnO₂ system showed no explicit sign for crystallite Pd, PdO or/and PdO₂ but, more probably 400°C is sufficiently able to oxidize palladium when chloride is involved. The oxidation was clearly shown in XRD data when film was prepared by PdCl₂ solution. The undetected signal of PdO/PdO₂ in PdO_x-SnO₂ films by X-ray diffractometer was probably due to the low amount of PdO_x loaded in the crystallite SnO₂ or/and due to a homogeneous distribution of PdO_x particles. Additionally, it could be predicted that the main recorded diffraction peak for PdO, which is located at $2\theta = 33.9^\circ$, is probably get overlapped with the highest intensity peak of SnO₂ at $2\theta = 33.6^\circ$.

The excellent improvement in sensor response and operating temperature that PdO_x-SnO₂ showed, is probably due to the smaller particles size and using the catalyst Pd as a dopant. Particles with smaller size possess a higher surface to volume ratio which increases the number of surface sites and as sequence, metal oxide will hosted more pre-chemisorbed oxygen. Additionally, using Pd as a dopant could increase the sensor response against H₂ and reduce the operating temperature of the sensor [23,24]. The achievement of the smaller size in our PdO_x-SnO₂ film may be related to our critical experimental technique. Usually, gas sensor subjected to pre-treatments in order to improve adhesion of sensing material with substrate

Table 1. Gives reported data of room temperature H₂ sensors, using different technologies

Methods	Synthesis method	Particle size (nm)	Operating Temp. (°C)	Functional material	Response (R _a /R _g) / ppm	Minimum concentration (ppm)	Humidity effect	Selective against	Electrodes
The Present work	SSTD	2-5	25	PdO _x /SnO ₂	5/ 300	< 4	10%change in resistance with no change in response	LPG,CO,CO ₂ , acetone, methanol and ethanol	Ag
The Present work	SSTD	2-5	50	PdO _x /SnO ₂	400/300	0.5	No effect	LPG,CO,CO ₂ , acetone, ethanol, methanol	Ag
[4]	Molecular Beam Epitaxy	30–150 nm.	RT	Pd/ZnO	1.05/250	10	-	-	Al/Ti/Au
[5]	vacuum-filtration process		20	Pd/Graphene	1.67/1000	40	-	-	
[6]	thermal vaporization process	<10 -<100	RT	Pd/SnO ₂	1.1/40	40	-	-	Ti/Au
[7]	Sol-Gel	20 nm	30	Pd/WO ₃	24000/13000	-	-	-	Ti/Au
[8]	metalorganic chemical vapor deposition		25	Pt/InN	1.04/300	20	-	-	Ti/Au
[9]	CVD	1-2 Tube size pd<5nm	RT	Pd /Carbon tube	1.03/30, 1.58/1000	30	-	-	Ti/Pd
[10]	electrodeposition	70-85 nm	RT	Pd single nanowire	1.0073/1000	-	-	-	Ti/Au
[11]	catalyst-free		25	SnO ₂	1.75/20000	-	-	-	RuO ₂ /Au
[12]	DC magnetron sputtering		20	Pd/Mg ₂ Ni	1.0054/1000	10	-	-	-
[14]	Sol-Gel	34 nm	RT	SnO ₂	0.67/3	3	-	-	Pd
[15]	lithographically patterned Pd nanowire electrodeposition	150 nm	RT	Pt-PdO nanowire	1.14/10	10	-	-	Au
[16]	magnetron sputtering method	-	RT	Pd/SnO ₂ /SiO ₂ /Si		0.5%	-	-	Pd/Si

and/or stabilize its resistance. This step, notably, increases the size of particles and in sequence sensor response decreases. Unlike other methods (SSTD method) required only one thermal step to synthesis and fabricate metal oxide film for sensing application.

Hydrogen (reducing gas) reacts most effectively with the pre-adsorbed oxygen on metals oxides at particular temperatures. This reaction results in the significant decrease in the resistance (R) of the sample due to formation of H₂O associated with electron(extracted by the per-adsorbed oxygen) going back to the conduction band of SnO₂. Also, it is expected that when hydrogen is exposed to the surface of PdO_x-SnO₂ sensor, probably Pd particles reacts quickly to form palladium hydride (PdH_x) [25]. The hydride has lower work function than pure Pd and could be considered as starting reaction of H₂ with PdO_x to form Pd as meta-stable state at lower operating temperatures [26]. H₂, also may get dissociated into hydrogen atoms by Pd metal resulting in transferring more electrons from the Pd film to SnO₂ film [27]. The dissociated hydrogen atoms are probably defused into sample and easily reacted with the pre-adsorbed oxygen species on SnO₂ surface. The dissociating step of hydrogen, in case of bare SnO₂ and PdO, is occurring at high temperature and may be considered as the first step of the reaction between the pre-adsorbed oxygen species in metal oxide and hydrogen atoms.

The reported available data, of hydrogen sensor works at room temperature (20-30°C) using different materials prepared with different synthesis methods and technologies, is summarized in Table 1. All the data of sensor response are converted to R_{air}/R_{H_2} . The minimum hydrogen concentration that recorded for the present sensor was found to be < 4 ppm at operating temperature of 25°C (Fig. 3b) and 0.5 ppm at operating temperatures of 50°C (Fig. 4a). These values are lower than the reported values in the literature (Table 1). These lower concentrations that our sensor could detect can be ascribed to the smaller particle size of sensing materials that was seen by TEM. The reported hydrogen sensors worked at RT (Table 1) have no available data of sensor selectivity while the present hydrogen sensor showed high selectivity against LPG, CO, CO₂, acetone, ethanol and methanol vapor (Fig. 4c). Also, as humidity is considered to be unavoidable agent, there is no data available of humidity effect on the available reported hydrogen sensors (Table 1). The

present sensor showed no effect of humidity on sensor response at sensor working temperature (25°C, 50°C and 80°C) which could be ascribed to the modification PdO_x in SnO₂ film. The reported sensor electrodes were mostly made of Ti and Au which are comparably costly; therefore silver (Ag) electrodes were used in our sensor as a part of simplicity of our sensor. The above comparison points could make our sensor a promising hydrogen sensor for industrial applications.

4. CONCLUSION

Simple method with, short processing time taken, no lithography, no vacuum required in sensor preparation, was used to prepare thin film hydrogen resistive sensor. The Pd additive increases the response and decreases the optimal operating temperature of SnO₂ sensor. The PdO_x-SnO₂ sensor could sense lesser than 4 ppm H₂ at RT with response of (1.62). The optimal operating temperature of the sensor was found to be 50°C where the sensor could sense 0.5 ppm of hydrogen. The sensor showed a response and recovery time was 4 and 9 sec respectively and no effective change in response with different relative humidity (20-90%). The sensor selectivity against LPG, CO, CO₂, acetone, methanol and ethanol is excellent. Because of sensor high reproducibility and selectivity a long with the wide active region (0.7-3000 ppm hydrogen), we think that PdO_x-SnO₂ thin films with silver electrodes, are supposed to be candidates for a low-cost room temperature hydrogen sensor.

DISCLAIMER

The products used for this research are commonly and predominantly use products in our area of research and country. There is absolutely no conflict of interest between the authors and producers of the products because we do not intend to use these products as an avenue for any litigation but for the advancement of knowledge. Also, the research was not funded by the producing company rather it was funded by personal efforts of the authors.

ACKNOWLEDGEMENT

Salim Bamsaoud is grateful to Al-awn foundation for their support to establish the center for natural and applied sciences at Hadhramout foundation for invention and advancement of sciences, Mukalla, Yemen.

COMPETING INTERESTS

Authors have declared that no competing interests exist.

REFERENCES

- Mubeen S, Zhang T, Yoo B, Deshusses MA, Myung NV. Palladium nanoparticles decorated single-walled carbon nanotube hydrogen sensor. *J. Phys. Chem C*. 2007;111(17):6321–7. Available: <https://doi.org/10.1021/jp067716m>
- Chen DA, Wang JJ, Xu Y. Hydrogen sensor based on Pd-functionalized film bulk acoustic resonator. *Sensors Actuators B Chem*. 2011;159(1):234–7. Available: <https://doi.org/10.1016/j.snb.2011.06.078>
- Bamsaoud SF, Rane SB, Karekar RN, Aiyer RC. Nano particulate SnO₂ based resistive films as a hydrogen and acetone vapour sensor. *Sensors Actuators B Chem*. 2011;153(2):382–91. Available: <https://doi.org/10.1016/j.snb.2010.11.003>
- Fields LL, Zheng JP, Cheng Y, Xiong P. Room-temperature low-power hydrogen sensor based on a single tin dioxide nanobelt. *Appl. Phys. Lett*. 2006;88(26):263102. Available: <https://doi.org/10.1016/j.jhydene.2020.06.136>
- Johnson JL, Behnam A, Pearton SJ, Ural A. Hydrogen sensing using Pd-functionalized multi-layer graphene nanoribbon networks. *Adv. Mater*. 2010;22(43):4877–80. Available: <https://doi.org/10.1002/adma.201001798>
- Lee JM, Park JE, Kim S, Kim S, Lee E, Kim SJ, Lee W. Ultra-sensitive hydrogen gas sensors based on Pd-decorated tin dioxide nanostructures: Room temperature operating sensors. *Int J Hydrogen Energy*. 2010;35(22):12568–73. Available: <https://doi.org/10.1016/j.jhydene.2010.08.026>
- Fardindoost S, Irajizad A, Rahimi F, Ghasempour R. Pd doped WO₃ films prepared by sol-gel process for hydrogen sensing. *Int. J. Hydrogen Energy*. 2010;35(2):854-860. Available: <https://doi.org/10.1016/j.jhydene.2009.11.033>
- Lim W, Wright JS, Gila BP, Pearton SJ, Ren F, Lai W-T, Chen L-C, Hu M-S, Chenn K-H. Selective-hydrogen sensing at room temperature with Pt-coated InN nanobelts. *Appl Phys Lett*. 2008;93(20):202109. Available: <https://doi.org/10.1063/1.3033548>
- Sun Y, Wang HH. High-performance, flexible hydrogen sensors that use carbon nanotubes decorated with palladium nanoparticles. *Adv. Mater*. 2007;19(19):2818–23. Available: <https://doi.org/10.1002/adma.200602975>
- Im Y, Lee C, Vasquez RP, Bangar MA, Myung NV, Menke EJ, Reginald M, Penner Prof. RM, Yun Prof. M. Investigation of a single Pd nanowire for use as a hydrogen sensor. *Small*. 2006;2(3):356–8. Available: <https://doi.org/10.1002/smll.200500365>
- Wang H-T, Kang BS, Ren F, Tien L-C, Sadik PW, Norton DP, Pearton SJ. Hydrogen-selective sensing at room temperature with ZnO nanorods. *Appl Phys Lett*. 2005;86(24):243503. Available: <https://doi.org/10.1063/1.1949707>
- Yoshimura K, Yamada Y, Okada M, Tazawa M, Jin P. Room-temperature hydrogen sensor based on Pd-capped Mg₂Ni thin film. *Jpn. J. Appl Phys*. 2004;43(4B):L507.
- Bamsaoud SF, Rane SB, Karekar RN, Aiyer RC. SnO₂ film with bimodal distribution of nano-particles for low concentration hydrogen sensor: Effect of firing temperature on sensing properties. *Mater. Chem. Phys*. 2012;133(2-3):681-687. Available: <https://doi.org/10.1016/j.matchemphys.2012.01.052>
- Kadhim IH, Abu Hassan H, brahim FT. Hydrogen gas sensing based on nanocrystalline SnO₂ thin films operating at low temperatures. *International Journal of Hydrogen Energy*; 2020. Available: <https://doi.org/10.1016/j.jhydene.2020.06.136>
- Cho HJ, Chen VT, Qiao S, Koo WT, Penner RM, Kim ID. Pt nanofunctionalized PdO nanowires for room temperature hydrogen gas sensors. *ACS Sensors*. 2018;3(10):2152-2158.

- Available:<https://doi.org/10.1021/acssensors.8b00714>
16. Wang F, Hu K, Liu H, Zhao Q, Wang K, Zhang Y. Low temperature and fast response hydrogen gas sensor with Pd coated SnO₂ nanofiber rods. *International Journal of Hydrogen Energy*. 2020;45(11): 7234-7242.
Available:<https://doi.org/10.1016/j.ijhydene.2019.12.152>
 17. Tan RQ, Guo YQ, Zhao JH, Li Y, Xu TF, Song WJ. Synthesis, characterization and gas-sensing properties of Pd-doped SnO₂ nano particles. *Trans Nonferrous Met Soc China*. 2011;21(7):1568–73.
Available:[http://dx.doi.org/10.1016/S1003-6326\(11\)60898-4](http://dx.doi.org/10.1016/S1003-6326(11)60898-4)
 18. Luo S, Fu G, Chen H, Liu Z, Hong Q. Gas-sensing properties and complex impedance analysis of Ce-added WO₃ nanoparticles to VOC gases. *Solid State Electron*. 2007;51(6):913–9.
Available:<https://doi.org/10.1016/j.sse.2007.04.010>
 19. Ansari SG, Borojerdian P, Sainkar SR, Karekar RN, Aiyer RC, Kulkarni SK. Grain size effects on H₂ gas sensitivity of thick film resistor using SnO₂ nanoparticles. *Thin Solid Films*. 1997;295(1–2):271–6.
Available:[https://doi.org/10.1016/S0040-6090\(96\)09152-3](https://doi.org/10.1016/S0040-6090(96)09152-3)
 20. Dharmadhikari AK, Kumbhojkar N, Dharmadhikari JA, Mahamuni S, Aiyer RC. Studies on third-harmonic generation in chemically grown ZnS quantum dots. *J Phys Condens Matter*. 1999;11(5):1363.
 21. Kumbhojkar N, Nikesh VV, Kshirsagar A, Mahamuni S. Photophysical properties of ZnS nanoclusters. *J. Appl. Phys*. 2000;88(11):6260.
Available:<http://scitation.aip.org/content/aip/journal/jap/88/11/10.1063/1.1321027>
 22. Zhang H, Li Z, Liu L, Xu X, Wang Z, Wang W, Zheng W, Dong B, Wang C. Enhancement of hydrogen monitoring properties based on Pd–SnO₂ composite nanofibers. *Sensors Actuators B Chem*. 2010;147(1):111–5.
Available:<https://doi.org/10.1016/j.snb.2010.01.056>
 23. Cha KH, Park HC, Kim KH. Effect of palladium doping and film thickness on the H₂-gas sensing characteristics of SnO₂. *Sensors Actuators B Chem*. 1994;21(2): 91–6.
Available:[https://doi.org/10.1016/0925-4005\(94\)80009-X](https://doi.org/10.1016/0925-4005(94)80009-X)
 24. Shen YB, Yamazaki T, Liu ZF, Meng D, Kikuta T. Hydrogen sensing properties of Pd-doped SnO₂ sputtered films with columnar nanostructures. *Thin Solid Films*. 2009;517(21):6119–23.
Available:<https://doi.org/10.1016/j.tsf.2009.05.036>
 25. Ling C, Xue Q, Han Z, Lu H, Xia F, Yan Z, Deng L. Room temperature hydrogen sensor with ultrahigh-responsive characteristics based on Pd/SnO₂/SiO₂/Si heterojunctions. *Sensors and Actuators B: Chem*. 2016;227:438-447.
Available:<https://doi.org/10.1016/j.snb.2015.12.077>
 26. Tsang SC, Bulpitt CDA, Mitchell PCH, Ramirez-Cuesta AJ. Some new insights into the sensing mechanism of palladium promoted tin (IV) oxide sensor. *J. Phys. Chem. B*. 2001;105(24):5737–42.
Available:<https://doi.org/10.1021/jp010175a>
 27. Salomonsson A, Eriksson M, Dannetun H. Hydrogen interaction with platinum and palladium metal-insulator-semiconductor devices. *J. Appl. Phys*. 2005;98(1):14505.
Available:<https://doi.org/10.1063/1.1953866>

© 2020 Bamsaoud et al.; This is an Open Access article distributed under the terms of the Creative Commons Attribution License (<http://creativecommons.org/licenses/by/4.0>), which permits unrestricted use, distribution, and reproduction in any medium, provided the original work is properly cited.

Peer-review history:
The peer review history for this paper can be accessed here:
<http://www.sdiarticle4.com/review-history/58663>